

Noninvasive Monitoring of Small Intestinal Oxygen in a Rat Model of Chronic Mesenteric Ischemia

Elaine M. Fisher · Mahmood Khan ·
Ronald Salisbury · Periannan Kuppusamy

Published online: 1 May 2013
© Springer Science+Business Media New York 2013

Abstract We noninvasively monitored the partial pressure of oxygen (pO_2) in rat's small intestine using a model of chronic mesenteric ischemia by electron paramagnetic resonance oximetry over a 7-day period. The particulate probe lithium octa-*n*-butoxynaphthalocyanine (LiNc-BuO) was embedded into the oxygen permeable material polydimethyl siloxane by cast-molding and polymerization (Oxy-Chip). A one-time surgical procedure was performed to place the Oxy-Chip on the outer wall of the small intestine (SI). The superior mesenteric artery (SMA) was banded to $\sim 30\%$ of blood flow for experimental rats. Noninvasive measurement of pO_2 was performed at the baseline for control rats or immediate post-banding and on days 1, 3, and 7. The SI pO_2 for control rats remained stable over the 7-day period. The pO_2 on day-7 was 54.5 ± 0.9 mmHg (mean \pm SE). SMA-banded rats were significantly different from controls with a noted reduction in pO_2 post banding with a progressive decline to a final pO_2 of 20.9 ± 4.5 mmHg (mean \pm SE; $p = 0.02$). All SMA-banded rats developed adhesions around the Oxy-Chip, yet remained asymptomatic. The hypoxia marker HypoxyprobeTM was used to validate the low tissue pO_2 . Brown cytoplasmic staining was consistent with hypoxia.

Mild brown staining was noted predominantly on the villus tips in control animals. SMA-banded rats had an extended region of hypoxic involvement in the villus with a higher intensity of cytoplasmic staining. Deep brown stainings of the enteric nervous system neurons and connective tissue both within layers and in the mesentery were noted. SMA-banded rats with lower pO_2 values had a higher intensity of staining. Thus, monitoring SI pO_2 using the probe Oxy-Chip provides a valid measure of tissue oxygenation. Tracking pO_2 in conditions that produce chronic mesenteric ischemia will contribute to our understanding of intestinal tissue oxygenation and how changes impact symptom evolution and the trajectory of chronic disease.

Keywords LiNc-BuO · EPR oximetry · Intestinal oxygenation · Superior mesentery artery occlusion · Chronic mesenteric ischemia

Introduction

Oxygen plays a central role in the pathogenesis of disease [1, 2]. Conditions such as chronic mesenteric ischemia, congestive heart failure (CHF), and bowel obstruction caused by adhesions or cancer reduce blood flow, and hence, oxygen delivery to the intestine. Reduced oxygen delivery to the gastrointestinal (GI) tract has been linked to the development of clinical symptoms such as abdominal pain, nausea and vomiting, bowel dysfunction, cachexia, malnutrition, and more seriously, the complications of sepsis, shock, and death [3, 4]. Clinical methods to detect intestinal oxygen are often employed when late symptoms of pain or longstanding GI distress are reported by the patient [5, 6]. At that moment, disease progression has occurred, and treatment has been delayed, leading to an

E. M. Fisher (✉)
School of Nursing, The University of Akron,
Akron, OH 44325, USA
e-mail: efisher@uakron.edu

M. Khan · P. Kuppusamy
Davis Heart and Lung Research Institute, The Ohio State
University, Columbus, OH 43210, USA

R. Salisbury
Department of Biology, The University of Akron,
Akron, OH 44325, USA

exacerbation of symptoms and potentially poorer patient outcome. As a first step toward understanding this process in the clinical setting, we seek to develop a noninvasive method to detect changes in intestinal oxygenation using a clinically relevant model of chronic mesenteric ischemia in rats. Detecting the changes in chronic intestinal pO_2 would allow for the early identification and implementation of pharmacological/nutraceutical treatments to prevent, limit, or modify disease progression. This study examined the noninvasive, site-specific detection of small intestinal pO_2 via electron paramagnetic resonance (EPR) oximetry using the polydimethyl siloxane (PDMS)-embedded lithium octa-*n*-butoxynaphthalocyanine (LiNc-BuO) probe, Oxy-Chip, over a 7-day period. In addition, the link between changes in oxygen trends and symptoms was investigated.

Materials and Methods

Ethical Approval

Animal experiments were conducted in accordance with the guiding Principles for the Care and Use of Laboratory Animals and Institutional Animal Care and Use Committee approved protocol (IACUC—The Ohio State University, Columbus, OH). Ten male Wister rats, three control and seven experimental, weighting 375–425 g were used in this study.

Surgical Preparation

Rats were anesthetized via an intraperitoneal injection of 200 mg/kg ketamine and 4 mg/kg xylazine. Toe pinch was used to ensure the depth of anesthesia with the aim at preventing movement. In the event of movement, a 1–1.5 % isoflurane/medical air (21 % O_2) mixture was delivered by nose cone. The abdomen was shaved and disinfected with 70 % povidone iodine. Under sterile conditions, a 5-cm midline incision was made. A $1.5 \times 0.25 \times 0.25$ cm strip of PDMS-embedded LiNc-BuO was placed in a plastic sling. The sling was then wrapped around the small intestine of ~ 10 cm above the cecum and sutured loosely along the edge border to hold the Oxy-Chip against the outer intestinal wall. The incision was sutured closed in two layers using 4–0 polypropylene. Temperature was maintained at 37 ± 1 °C using an infrared heat lamp. EPR measurement was carried out when the rat remained anesthetized. Animals were recovered until fully awake and moving. A one-time dose of buprenorphine (0.5 mL; 0.015 mg/1 mL) was administered subcutaneously. Rats had free access to food and water and were returned to the animal facility when recovered.

Model of Chronic Mesenteric Ischemia

For the experimental group rats, the superior mesenteric artery (SMA) was isolated and banded by placing a blunt-tipped 25-gauge needle over the SMA, slightly beyond its origin from the abdominal aorta, and tying it with 5–0 nylon suture. The needle was then removed, and the constriction remained. We previously determined that SMA banding using a 25-gauge needle produced a reduction in SMA flow between 65 and 70 % of baseline. Using a Transonic Flowprobe (T-206, Transonic Systems Inc., Ithica, NY), baseline perfusion was 8.8 mL/min pre banding and 2.6–3 mL/min post SMA banding. When corrected to body weight, the baseline SMA perfusion rate was 22–26 mL/min/kg, consistent with the literature findings. Animal survival up to 7 weeks has been achieved using our SMA-banded model of 30–35 % perfusion. Henceforth, experimental rats with 30–35 % perfusion will be referred to as SMA-banded rats. SMA blood flow <25 % of baseline was consistent with extensive necrosis and death within 24–48 h of banding. For this study, we kept animals alive for 7 days.

Oxy-Chip

The Oxy-Chip is composed of sonicated LiNc-BuO microcrystals (1–10 μ) embedded in the oxygen-permeable material PDMS by cast molding and polymerization (40 mg LiNc-BuO in 5.5 g PDMS) [7–9]. LiNc-BuO is a nontoxic, particulate oxygen probe which has been extensively studied in vitro and in vivo [7, 10–12]. The LiNc-BuO probe has a very high spin density (7.2×10^{20}) and yields a single, sharp EPR absorption peak. In vivo biocompatibility was previously established by co-incubation with cultured cells [7]. In vivo the solid PDMS/LiNc-BuO chip, called Oxy-Chip, produced reliable and reproducible measures of rat muscle pO_2 under conditions of ischemia and hypoxia [7]. LiNc-BuO microcrystals alone as well as embedded in the PDMS chip demonstrate long-term stability, maintaining line shape and oxygen sensitivity for 2 months or more in vivo [7, 12, 13].

EPR Oximetry

L-band (1.2 GHz) EPR oximetry allows for noninvasive detection of pO_2 in live animals. The EPR line width is sensitive to changes in molecular oxygen with the peak-to-peak spectral width dependent on the oxygen concentration, e.g., 20.9, 0 % [12]. A linear relationship exists between the line width and oxygen concentration (pO_2) in the range of 0–760 mmHg suggesting that spin exchange increases linearly with pO_2 . Plotting the line width slope against the pO_2 curve for the oxygen-sensing probe

LiNc-BuO yields an oxygen sensitivity of the probe line width of 8.0 milligauss/mmHg. Sensitivity is calculated as the difference between room air O_2 and tissue anoxia, divided by O_2 at 1 ATM [12]. The tissue anoxic value, pO_2 37 mmHg, was determined by averaging 10 EPR spectra from euthanized rats 5 min after death.

EPR Oximetry Measurement

L-band (1.2 GHz) EPR spectroscopy (Bruker Biospin, Billerica, MA) was used to monitor intestinal pO_2 . For both control and experimental rats, the abdomen was closed, and the initial measures were obtained noninvasively. While our previous research demonstrated a reduction in pO_2 from baseline to post banding with the abdomen open, this value may have been spuriously high because of environmental oxygen exchange. Because we chose to perform all pO_2 measures noninvasively, abdomen closed, we did not perform the baseline pO_2 measurement before SMA banding. EPR spectra were obtained on days 0 (baseline), 1, 3, and 7 at about the same time daily to avoid the impact of physiological variations in biorhythms, and physiological and psychological stresses on the rat. Measurement protocol involved anesthetizing the rat using induction isoflurane (2–3 %) followed by a maintenance dose of 0.5–1.5 % via nose cone to prevent movement. Rats were secured in a supine position to a bedplate with adhesive tape. The surface coil resonator was brought into contact with the skin. Because of the motility of the intestine, the resonator position was adjusted until spectra could be obtained indicating that the resonator was positioned directly over the Oxy-Chip. EPR spectra were obtained using customized data acquisition software and by averaging five cycles of measurement to obtain a single value over 2–3 min.

Tissue Hypoxia Evaluation

To evaluate the validity of EPR pO_2 measurement, pimonidazole hydrochloride (HypoxyprobeTM-1; HPI, Inc., Burlington, MA), a 2-nitroimidazole immunochemical hypoxia marker was used. For cells with a pO_2 <10 mmHg, the 2-nitroimidazole irreversibly binds to the thiol groups in proteins to form intracellular adducts. These protein adducts are effective immunogens for the production of monoclonal and polyclonal antibodies. The monoclonal antibody IgG₁ (HypoxyprobeTM-1Mab1) was used to detect hypoxic cells with pO_2 values <10 mmHg by staining the cytoplasm within cells brown.

Termination Protocol

After the final EPR measurement on day 7, an intraperitoneal injection of sodium pentobarbital (50 mg/mL;

0.8 mL) was administered. The sedated rat was given an intravenous injection of HypoxyprobeTM-1 (60 mg/kg) which circulated for 15 min. Next, the abdomen was reopened, and the SI was excised 1 cm above and below the Oxy-Chip. Tissue was preserved in 4 % formalin for histologic analysis. The rat was euthanized by diaphragm puncture. The formalin-preserved tissues were embedded in paraffin and stained with hematoxylin–eosin (H & E). Also, tissues were processed using the peroxidase immunohistochemistry technique, the recommended procedure for immunostaining Hypoxyprobe-1 adducts using paraffin-embedded tissues (HypoxyprobeTM-1 Plus Kit for the Detection of Tissue Hypoxia, HPI, Inc.). A 1:100 dilution (150 μ l) of Hypoxyprobe-1Mab was added to each section. Histologic evaluation was done under light microscopy. The intensity of brown staining within the small intestine indicated the extent of tissue hypoxia.

Statistical Methods

Repeated-measures ANOVA was used to compare changes in pO_2 between the control and SMA-banded rats (baseline-day 0, 1, 3, and 7). Analyses were performed using SPSS 15.0 for Windows. Data are reported as mean \pm SE. The level of significance was set at $p < 0.05$.

Results

Oxy-Chip and SI Wall Contact at day-7

We achieved our goal of site-specific monitoring of SI wall pO_2 . On necropsy, we visually confirmed Oxy-Chip contact with the external SI wall in all rats on day 7. A thin biofilm formed on the outside of the Oxy-Chip which held the chip in direct contact with the serosal surface. The plastic sling was not biocompatible and provoked an inflammatory response along the border edges as evidenced by erythema of the intestinal wall. Using light microscopy, H & E-stained tissue revealed increased infiltration of WBCs throughout the intestinal connective tissue. In the connective tissue of the mesentery, outside of the serosal layer, larger numbers of fibroblasts were found. For SMA-banded rats, the finding of larger numbers of fibroblasts paralleled the incidence of adhesion formation.

Oxygen Trends and Symptom Development

All control rats ($n = 3$) and six of the seven rats in the SMA-banded group maintained normal activity, grooming, and feces. Necropsy on day 7 for the control animals revealed a hyperemic inflammatory tissue response at the edges of the plastic sling where mechanical irritation had

occurred. No adhesions were noted for control rats at the Oxy-Chip site. Local peritoneal adhesions were found in all the SMA-banded rats in the area of Oxy-Chip placement. Using an adhesion grading scale, all adhesions were Grade 2, defined as firm with limited vascular adhesions and separated by aggressive blunt dissection [14]. On day 6, one rat appeared ill with lower grooming and activity and diarrhea. This rat was immediately euthanized. Necropsy revealed a 10-cm section of small intestinal necrosis with generalized whole bowel hyperemia and dilated, gas-filled intestinal loops. The pO_2 values for this rat were 33.1, 50.6, 33.8, and 4.4 mmHg on days 0 (post-banding), 1, 3, and 6, respectively.

Oxy-Chip pO_2 Measurement

Spectra obtained over a 5-min period were averaged to produce a single value at each time point. Because of intestinal motility, rats had to be repositioned multiple times until the resonator was directly over the Oxy-Chip to obtain the spectrum. On two occasions, in two different rats, the EPR spectrum was unable to be detected. Figures 1 and 2 illustrate individual rat data points for the control and SMA-banded pO_2 values over the 7-day protocol. Average pO_2 values (mean \pm SE) by groups are depicted in Fig. 3. There was a nonsignificant increase in the measured pO_2 values on day 1, which stabilized by days 3 and 7 for the control animals ($n = 3$). There were no significant differences in SI pO_2 values in the control rats over the 7-day period. The SMA-banded rats ($n = 6$) demonstrated a similar nonsignificant increase in pO_2 on day 1 from immediate postbanding values, followed by a progressive reduction in pO_2 values on days 3 and 7, respectively. No within-group differences were noted

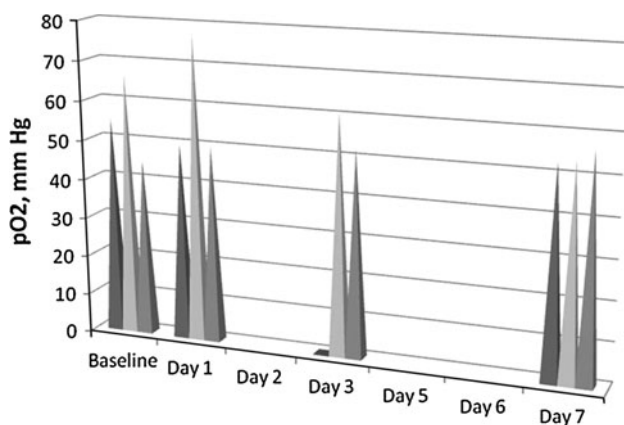


Fig. 1 Measured pO_2 in control rats. Spikes represent individual pO_2 values for control rats ($n = 3$) at baseline, days 1, 3, and 7. On day 1 a slight increase in pO_2 was noted. The small circle in position one on day 3 represents our inability to locate the probe and obtain the EPR measurement. The pO_2 was stable for the three control rats on day 7

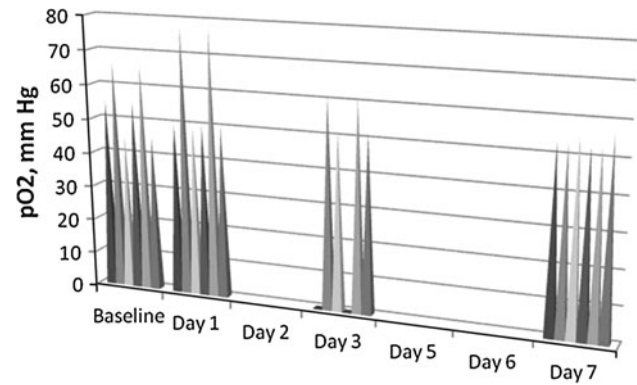


Fig. 2 Measured pO_2 in SMA-banded rats. Spikes represent individual pO_2 values for SMA-banded rats ($n = 6$) immediately post-banding after the abdomen was closed and on days 1, 3, and 7. A nonsignificant rise in pO_2 was noted for some rats on day 1 followed by a progressive decline in pO_2 to day 7. On day 1 we were unable to locate the probe for EPR measurement. No significant difference in pO_2 was found from baseline banding to day 7. When control baseline values were used, a significant decline in pO_2 was detected on day 7 ($p < 0.05$)

during the 7-day period. Analysis using repeated-measures ANOVA resulted in the mean pO_2 differences between the control and the SMA-banded groups ($p = 0.02$). The O_2 % of small intestinal tissues under the baseline control conditions were 7.8 and 7.6 % on day 7. Upon postbanding, the average O_2 % was 4.4 % with a decline to 3.2 % on day 7.

Histology and Tissue Hypoxia Assay

Histology samples representative of the control and the SMA-banded rats are displayed in Fig. 4. Layers of the intestine in both the groups were consistent with the normal architecture of ileal tissue. Villus height was similar for the study groups. HypoxyprobeTM staining was noted at the villus tips of the control animals with larger regions of villus involvement and intensity of brown staining noted for the SMA-banded animals. Neurons of the enteric nervous system in both Auerbach's and Meissner's plexus stained dark brown in the SMA-banded group. Although it is not displayed in Fig. 4, we confirmed staining of the hypoxic neuronal cells and ruled out artifact and HypoxyprobeTM staining of satellite or connective tissue cells. Inter-rat variability in the intensity of brown staining for the SMA-banded group was consistent with the level of pO_2 . Rats with a final EPR-measured pO_2 values < 10 mmHg, had a high intensity of brown staining of the villus when compared with rats with the measured pO_2 values > 30 mmHg. The villus staining in SMA-banded rats with pO_2 values > 30 mmHg had brown staining similar to the control rats. For rats with a final $pO_2 < 10$ mmHg, dark brown cytoplasmic staining of connective tissue in the

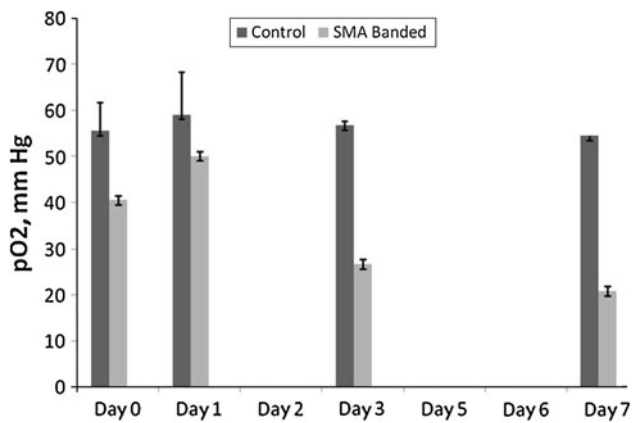


Fig. 3 Comparison of mean pO₂ for control and SMA-banded rats. A significant difference between mean pO₂ was found between control and SMA-banded rats, $p = 0.02$. No within group differences were found for control or SMA-banded rats. Data are reported as mean \pm SE

lamina, submucosa, muscle layers, and mesentery was observed.

Discussion

Oxygen Results

Accurate and reliable noninvasive site-specific monitoring of SI pO₂ is possible in rodent models using the Oxy-Chip probe measured by EPR oximetry. The clinically simulated rat model of chronic ischemia, with the SMA-banding being 30–35 % of baseline perfusion, allowed us to track changes in SI pO₂ over a 7-day period. The intestine is sensitive to changes in oxygenation by ischemia. A preponderance of reported studies focused on acute, ischemic-reperfusion injury (I/R). A higher degree of SI injury is reported for I/R injury than when injury results from ischemia alone [15]. One possible explanation for this difference relates to the greater oxidative stress and the generation of free radicals during reperfusion [4, 16].

Intestinal pO₂ measured using a polarographic oxygen electrode placed in direct contact with the serosa of the ileum yielded baseline results similar to those of this study, 52 ± 8 [17] versus 55.5 ± 11 mmHg. The pO₂ on day 1 increased for the majority of the control and SMA-banded rats. Two explanations are posed for this finding. First, we hypothesize an oxidative burst by neutrophils resulting from surgery to raise pO₂. Greater neutrophil mobilization and neutrophil stress result in enhanced production of reactive oxygen species (ROS) [18] with neutrophil mobilization being a more important contributor to ROS generation, particularly during I/R [19]. While our model was not an I/R model, we did produce transient total

occlusion of the SMA artery during banding followed by reperfusion as we opened the vessel by removing our needle. Cizova et al. demonstrated a significant increase in neutrophils from baseline after 15–30 min I/R. Following ischemia only, they reported neutrophil counts similar to baseline [19]. With our model of chronic small intestinal ischemia, we would expect higher oxidative stress and tissue damage to develop over time.

A second hypothesis for the rise in pO₂ on day 1 relates to compensatory flow-mediated dilation and hyperemia in response to surgical manipulation. Compensatory hyperemic is a regulatory response at the microvascular level to ischemia. ROS stimulated the release of local vasodilating substances such as adenosine, endothelium derived nitric oxide [20], and other nonendothelium dependent vasodilators promoted microvessel perfusion [21, 22]. In our SMA-banded model, we did not band the celiac artery. The release of local vasodilator substances may have initially enhanced circulation through the celiac artery. Variability of outcome postSMA banding is noted in studies when other routes of circulation have not been simultaneously occluded. For our study, survival was necessary, and hence we may not have simulated a total blood flow scenario of 30–35 % reduction in blood flow overall; however, flow reduction by partial occlusion of the SMA was sufficient to create a clinically relevant model of chronic ischemia. Thus, we hypothesize that the transient rise in pO₂ on day 1 could be explained by neutrophil oxidative burst and a microvascular compensatory response triggered by surgical manipulation and banding.

Validation of pO₂ with HypoxyprobeTM

HypoxyprobeTM is a marker of hypoxia used to qualitatively validate changes in tissue/organ oxygenation. Hundreds of studies in the literature have reported using this probe to evaluate hypoxic gradients in tumors as well as solid organs, e.g., liver and kidney in vitro and in vivo for animals and humans. HypoxyprobeTM irreversibly binds to hypoxic cells with an oxygen tension of <10 mmHg and produces a deeper brown staining as the pO₂ declines. HypoxyprobeTM was a better marker than HIF-1 alpha for our application since it predominantly binds to chronic hypoxic cells [23].

In the SMA-banded rats we anticipated extensive chronic hypoxic changes in enterocytes by nature of their high metabolic activity, unique countercurrent exchange mechanism to oxygenate the intestinal villus, and turnover rate. The ileum of the SI is an active site for nutrient absorption, and thus, vulnerable to changes in oxygenation. Blood flow to the villus tips is influenced by countercurrent exchange [24]. As oxygen is exchanged across the artery and vein in response to tissue metabolic needs, a progressive decrease

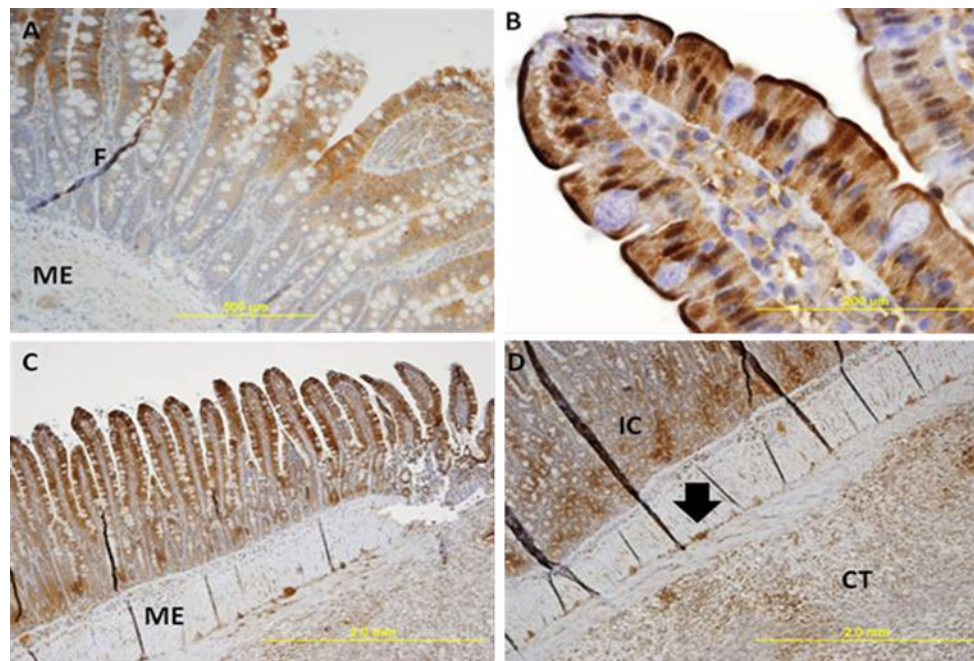


Fig. 4 In vivo comparison of pO_2 in control and SMA banded rats using Hypoxyprobe™. Images were obtained using light microscopy at different magnifications ($\times 4$, $\times 10$, $\times 20$, $\times 40$). All images are from ileal tissue. Figure **a** depicts an image in a control rat, while **b**, **c**, and **d** are SMA-banded rat images. Tissues are stained with Hypoxyprobe™ which binds to protein thiol groups in cells with oxygen tension <10 mmHg and produces a brown stain. Although a qualitative indicator of the degree of hypoxia, the color intensity of the brown stain relates to the degree of hypoxia with darker intensity interpreted as more hypoxic. Dark lines in the tissues represent tissue folds. A representative tissue fold is labeled as *F* in diagram **a**. The following letters mean: *CT* subserosal connective tissue, *IC* intestinal crypts, and *ME* muscularis externa. The closed arrow indicates the

myenteric plexus. Images: **a** villus tip staining in a control rat; **b** cytoplasmic staining by Hypoxyprobe™ of enterocytes on a villi tip; **c** a more extensive and deeper brown staining of the ileum; **d** a $\times 20$ magnification of the image displayed in (**c**). In this rat the EPR measured pO_2 was 7.5 mmHg. Brown stain is seen throughout the connective tissue of the submucosa, circular and longitudinal muscle, and the subserosal connective tissue noted as CT. The arrow indicates neuron hypoxia and further examination illustrates multiple sites of neuron death in all enteric nervous system cells. Not shown, on $\times 40$ magnification, both Auerbach's and Meissner's plexus hypoxia was prominent. We were able to rule out death in these areas being attributable to satellite cell death or connective tissue surrounding these neurons

in oxygen tension from base to top occurs. Blood flow at the villus base was been reported to differ by as much as 25 mmHg at the tips [25].

Normal cell turnover of the endothelial lining of the intestine occurs every 3.5 days [26, 27]. The turnover of enterocytes is precisely regulated by cell proliferation and apoptosis [28]. Beginning in the crypts of Lieberkühn, cells of different lineage, e.g., mucus-producing goblet cells, absorptive enterocytes, and enteroendocrine cells, are matured and migrate toward the villus tips where they will be sloughed or die by apoptosis. Our present histology results show that the villus tips in both the control and the SMA-banded groups stained positive with Hypoxyprobe™. More extensive villus involvement and deeper brown staining of the villus was found in the SMA-banded rats. The cytoplasmic staining of the villus in the control group may reflect normal cell turnover by apoptosis. A second possible explanation for the positive staining relates to the differences in anesthetic protocols used during EPR oximetry measurement and tissue harvesting, isoflurane

and pentobarbital, respectively. Studying the effect of varying anesthetics on tumors, Baudalet and Gallez [29] reported reduced oxygenation and flow to several tissue when pentobarbital was administered. Thus, we are constrained in our ability to explain the resultant tissue staining indicative of villus hypoxia in control rats.

Our results showed a greater area of villus involvement and higher intensity of cytoplasmic staining in the SMA-banded rats than in controls. For the SMA-banded rats with EPR-measured pO_2 values >30 mmHg immediately before tissue retrieval, the pattern of staining was similar to the control tissue, but with a higher intensity of brown color. This finding suggests a broader involvement of tissue hypoxia. In rats with EPR oximetry values <10 mmHg, in addition to the widespread villus involvement and darker staining, the neuronal cells in both Auerbach's and Meissner's plexuses were heavily stained. Extension of cell hypoxia to the connective tissue within the smooth muscle but not the muscle cells in either the circular or longitudinal layers, stained dark brown. What is unknown is the

effect that enteric nervous system neuronal hypoxia and the muscle and associated connective tissue have on intestinal function and symptoms development. HypoxyprobeTM was useful in this study to detect hypoxic gradients in chronic intestinal ischemia, which were consistent with reductions in the EPR-measured oxygen tension in the small intestine.

Adhesion Formation

All the SMA-banded rats developed peritoneal adhesions at the Oxy-Chip site. The peritoneum is composed of a loosely anchored, single outer layer of mesothelial cells. Trauma to the delicate mesothelium from the surgical handling and instrument contact results in the development of adhesions at 5–7 days post injury. Adhesion formation begins with coagulation that initiates a cascade of events leading to the buildup of a fibrin gel matrix that forms a bridge between two damaged peritoneal surfaces [30]. The release of proinflammatory cytokines IL-1, IL-6, IL-8, TNF- α , counteract the fibrinolytic system and promote adhesion formation [31–33].

In response to ischemia, free radical release leading to superoxide generation is thought to be the major trigger for adhesion development [34, 35]. The initial infiltration by polymorphonuclear leukocytes is followed on day 5–7 with infiltration by fibroblasts [36]. Hypoxia triggers normal peritoneal fibroblasts to irreversibly acquire an adhesion phenotype. The adhesion phenotype promotes increased production of the cytokine transforming growth factor beta (TGF- β 1) and Type I collagen. TGF- β 1 decreases peritoneal fibrinolytic capacity to dissolve fibrinous adhesions. When xanthine oxidase, a principal superoxide producing enzyme was inhibited, adhesion formation declined [37]. Thus, oxygen-derived free radicals may be pathogenically important to adhesion formation [38]. Our ischemic model likely produced adhesions by a combination of ischemia and inflammatory processes.

Limitations to SI pO₂ Monitoring

Oxygen-sensitive probes must be suited to their specific application. Despite successfully monitoring SI pO₂ for 7 days, we continued to encounter major obstacles to long-term monitoring of intestinal oxygenation. Two areas of continued challenge include probe placement and the need for a biocompatible material to attach the Oxy-Chip to the outer serosal wall. Probe placement for intestinal pO₂ monitoring presents a different set of challenges other than those for monitoring in solid organs. In tumors [39] and solid organs, such as the heart [11] or skeletal muscle [12], the direct implantation of LiNc-BuO microcrystals by injection is possible. Once placed, the LiNc-BuO probe remains in situ, and is easily located for subsequent EPR

measurement, making long-term pO₂ monitoring feasible. Khan et al. [11] reported placement of LiNc-BuO within the heart produced an inflammatory tissue reaction around the LiNc-BuO deposit, attributed most likely to the method of implantation which did not interfere with probe sensitivity.

Our research focuses on monitoring pO₂ of the SI because of its high metabolic activity and role in the digestion and absorption of nutrients. In prior experiments, we attempted to inject sufficient quantities of the LiNc-BuO microcrystals into the thin-wall of the small intestine. However, the majority of the injected LiNc-BuO was deposited inside the bowel lumen. Intraluminal pO₂ values were significantly lower than the SI tissue pO₂ reported in this study 9.6 mmHg versus 54.5 mmHg, respectively. Intestinal wall injection also runs the risk of accidental bowel perforation with ensuing peritonitis and sepsis. We were able to inject small quantities of LiNc-BuO between the layers of the large intestine. However, when the abdomen was closed, we were unable to locate the probe and, thus could not noninvasively measure intestinal oxygenation.

The more recently developed Oxy-Chip, used in this research study, provides a dense concentration of LiNc-BuO microcrystals embedded in PDMS [8]. The Oxy-Chip was cut in strips larger than necessary to obtain an EPR signal but of sufficient size to be able to locate the probe for monitoring when the abdomen was closed. The semi-rigid nature of the Oxy-Chip is a drawback for intestinal monitoring. The mechanical properties do not allow for the wrapping of the material around the intestine, and thus, the challenge of how to attach the probe to the surface of the intestine remains. Our initial attempt to make use of the Oxy-Chip for SI monitoring was by suturing the chip onto the peritoneal wall. Once the abdomen was closed, the Oxy-Chip lay in direct contact with the intestinal surface. After 1 week, our ability to obtain an EPR spectrum was sporadic. For rats euthanized at 1 month, a thick layer of abdominal fat had adhered to the probe surface. Thus, we likely measured fat and peritoneal muscle pO₂ instead of intestinal pO₂ (18.8–21.9 mmHg fat/muscle pO₂ versus 20.9 mmHg intestinal pO₂).

For the current experimental pilot study, we placed the semi-rigid Oxy-Chip against the intestinal wall using a sling that was slipped around the intestine and loosely sutured on top to hold the chip in direct contact with the intestine. The intestine is a motile organ with irritation from the thin plastic material used as a sling evident. In addition, the presence of greater number of WBCs within tissue was noted on H & E staining compared with normal ileal tissue samples (not shown). Interestingly, adhesions did not form in control animals, but extensive adhesion formation was observed in all the SMA-banded rats

suggesting the key role that the tissue hypoxia may play in adhesion formation. It is common knowledge that bowel ischemia occurs in the presence of adhesions, but what remains controversial is the role that ischemia plays in the formation of adhesions.

Conclusion

This research represents the first step toward realizing the aim of this study, namely, the noninvasive monitoring of chronic ischemic changes in SI pO₂ over time. Our study continues to develop and test methods for noninvasive SI pO₂ measurement using flexible, LiNc-BuO-embedded EPR-sensitive materials that are biocompatible and allow for site-specific pO₂ monitoring. Our long-term aim is toward clinical application. Currently, the clinical presentation of intestinal ischemia is variable, and appropriate clinical management remains controversial. Possessing the ability to track changes produced by chronic ischemia primarily in an animal model and ultimately in patients will contribute to our understanding of tissue oxygenation and how changes would impact symptom evolution and the trajectory of chronic disease. This study demonstrates preliminary success in tracking intestinal changes in oxygenation using EPR oximetry.

Acknowledgments This study was supported by a Career Training Award (K01-NR009787-01) from the National Institute of Health: National Institute of Nursing Research to E.M. Fisher. We thank Dr. Sheau-Huey Chiu for assistance with statistical analysis.

References

- Kulkarni, A. C., Kuppusamy, P., & Parinandi, N. (2007). Oxygen, the lead actor in the pathophysiologic drama: enactment of the trinity of normoxia, hypoxia, and hyperoxia in disease and therapy. *Antioxidants & Redox Signaling*, *9*, 1717–1730.
- Kutala, V. K., Khan, M., Angelos, M. G., & Kuppusamy, P. (2007). Role of oxygen in postischemic myocardial injury. *Antioxidants & Redox Signaling*, *9*, 1193–1206.
- Sandek, A., Bauditz, J., Swidsinski, A., Buhner, S., Weber-Eibel, J., von Haehling, S., et al. (2007). Altered intestinal function in patients with chronic heart failure. *Journal of the American College of Cardiology*, *50*, 1561–1569.
- Parks, D. A., Bulkley, G. B., Granger, D. N., Hamilton, S. R., & McCord, J. M. (1982). Ischemic injury in the cat small intestine: role of superoxide radicals. *Gastroenterology*, *82*, 9–15.
- Phillips, J. P., Kyriacou, P. A., Jones, D. P., Shelley, K. H., & Langford, R. M. (2008). Pulse oximetry and photoplethysmographic waveform analysis of the esophagus and bowel. *Current Opinion in Anaesthesiology*, *21*, 779–783.
- van Noord, D., Mensink, P. B., de Knegt, R. J., Ouwendijk, M., Francke, J., van Vuuren, A. J., et al. (2011). Serum markers and intestinal mucosal injury in chronic gastrointestinal ischemia. *Digestive Diseases and Sciences*, *56*(2), 506–512.
- Meenakshisundaram, G., Eteshola, E., Pandian, R. P., Bratasz, A., Selvendiran, K., Lee, S. C., et al. (2009). Oxygen sensitivity and biocompatibility of an implantable paramagnetic probe for repeated measurements of tissue oxygenation. *Biomedical Microdevices*, *11*, 817–826.
- Meenakshisundaram, G., Eteshola, E., Pandian, R. P., Bratasz, A., Lee, S. C., & Kuppusamy, P. (2009). Fabrication and physical evaluation of a polymer-encapsulated paramagnetic probe for biomedical oximetry. *Biomedical Microdevices*, *11*, 773–782.
- Eteshola, E., Pandian, R. P., Lee, S. C., & Kuppusamy, P. (2009). Polymer coating of paramagnetic particulates for in vivo oxygen-sensing applications. *Biomedical Microdevices*, *11*, 379–387.
- Khan, M., Kutala, V. K., Vikram, D. S., Wisel, S., Chacko, S. M., Kuppusamy, M. L., et al. (2007). Skeletal myoblasts transplanted in the ischemic myocardium enhance in situ oxygenation and recovery of contractile function. *American Journal of Physiology*, *293*, H2129–H2139.
- Khan, M., Kutala, V. K., Wisel, S., Chacko, S. M., Kuppusamy, M. L., Kwiatkowski, P., et al. (2008). Measurement of oxygenation at the site of stem cell therapy in a murine model of myocardial infarction. *Advances in Experimental Medicine and Biology*, *614*, 45–52.
- Pandian, R. P., Parinandi, N. L., Ilangovan, G., Zweier, J. L., & Kuppusamy, P. (2003). Novel particulate spin probe for targeted determination of oxygen in cells and tissues. *Free Radical Biology Medicine*, *35*, 1138–1148.
- Chacko, S. M., Khan, M., Kuppusamy, M. L., Pandian, R. P., Varadaraj, S., Selvendiran, K., et al. (2009). Myocardial oxygenation and functional recovery in infarct rat hearts transplanted with mesenchymal stem cells. *American Journal Physiology Heart Circulation Physiology*, *296*, H1263–H1273.
- Tarhan, O. R., Barut, I., Sutcu, R., Akdeniz, Y., & Akturk, O. (2006). Pentoxifylline, a methyl xanthine derivative, reduces peritoneal adhesions and increases peritoneal fibrinolysis in rats. *Tohoku Journal of Experimental Medicine*, *209*, 249–255.
- Wu, B., Qiu, W., Wang, P., Yu, H., Cheng, T., Zambetti, G. P., et al. (2007). p53 independent induction of PUMA mediates intestinal apoptosis in response to ischaemia-reperfusion. *Gut*, *56*, 645–654.
- Granger, D. N., Hollwarth, M. E., & Parks, D. A. (1986). Ischemia-reperfusion injury: role of oxygen-derived free radicals. *Acta Physiologica Scandinavica Supplement*, *548*, 47–63.
- Mellstrom, A., Mansson, P., Jonsson, K., & Hartmann, M. (2009). Measurements of subcutaneous tissue pO₂ reflect oxygen metabolism of the small intestinal mucosa during hemorrhage and resuscitation. An experimental study in pigs. *European Surgical Research*, *42*, 122–129.
- Yung, L. M., Leung, F. P., Yao, X., Chen, Z. Y., & Huang, Y. (2006). Reactive oxygen species in vascular wall. *Cardiovascular & Hematological Disorders*, *6*, 1–19.
- Cizova, H., Lojek, A., Kubala, L., & Ciz, M. (2004). The effect of intestinal ischemia duration on changes in plasma antioxidant defense status in rats. *Physiological Research*, *53*, 523–531.
- Meredith, I. T., Currie, K. E., Anderson, T. J., Roddy, M. A., Ganz, P., & Creager, M. A. (1996). Postischemic vasodilation in human forearm is dependent on endothelium-derived nitric oxide. *American Journal of Physiology*, *270*, H1435–H1440.
- Loscalzo, J., & Vita, J. A. (1994). Ischemia, hyperemia, exercise, and nitric oxide. Complex physiology and complex molecular adaptations. *Circulation*, *90*, 2556–2559.
- Huang, A. L., Silver, A. E., Shvenke, E., Schopfer, D. W., Jahangir, E., Titas, M. A., et al. (2007). Predictive value of reactive hyperemia for cardiovascular events in patients with peripheral arterial disease undergoing vascular surgery. *Arteriosclerosis, Thrombosis, and Vascular Biology*, *27*, 2113–2119.

23. Goethals, L., Debucquoy, A., Perneel, C., Geboes, K., Ectors, N., De Schutter, H., et al. (2006). Hypoxia in human colorectal adenocarcinoma: comparison between extrinsic and potential intrinsic hypoxia markers. *International Journal of Radiation Oncology Biology Physics*, *65*, 246–254.
24. Bohlen, H. G. (1998). Integration of intestinal structure, function, and microvascular regulation. *Microcirculation*, *5*, 27–37.
25. Bohlen, H. G. (1980). Intestinal mucosal oxygenation influences absorptive hyperemia. *American Journal of Physiology*, *239*, H489–H493.
26. Hall, P. A., Coates, P. J., Ansari, B., & Hopwood, D. (1994). Regulation of cell number in the mammalian gastrointestinal tract: the importance of apoptosis. *Journal of Cell Science*, *107*(Pt 12), 3569–3577.
27. Kerr, J. F., Wyllie, A. H., & Currie, A. R. (1972). Apoptosis: a basic biological phenomenon with wide-ranging implications in tissue kinetics. *British Journal of Cancer*, *26*, 239–257.
28. Potten, C. S., & Booth, C. (1997). The role of radiation-induced and spontaneous apoptosis in the homeostasis of the gastrointestinal epithelium: A brief review. *Comparative Biochemistry and Physiology Part B: Biochemistry and Molecular Biology*, *118*, 473–478.
29. Baudelet, C., & Gallez, B. (2004). Effect of anesthesia on the signal intensity in tumors using BOLD-MRI: comparison with flow measurements by Laser Doppler flowmetry and oxygen measurements by luminescence-based probes. *Magnetic Resonance Imaging*, *22*, 905–912.
30. Holmdahl, L., & Risberg, B. (1997). Adhesions: Prevention and complications in general surgery. *European Journal of Surgery*, *163*, 169–174.
31. Holmdahl, L., & Ivarsson, M. L. (1999). The role of cytokines, coagulation, and fibrinolysis in peritoneal tissue repair. *European Journal of Surgery*, *165*, 1012–1019.
32. Brauner, A., Hylander, B., & Wretling, B. (1993). Interleukin-6 and interleukin-8 in dialysate and serum from patients on continuous ambulatory peritoneal dialysis. *American Journal of Kidney Disease*, *22*, 430–435.
33. Brauner, A., Hylander, B., & Wretling, B. (1996). Tumor necrosis factor-alpha, interleukin-1 beta, and interleukin-1 receptor antagonist in dialysate and serum from patients on continuous ambulatory peritoneal dialysis. *American Journal of Kidney Disease*, *27*, 402–408.
34. Saed, G. M., Zhang, W., & Diamond, M. P. (2000). Effect of hypoxia on stimulatory effect of TGF-beta 1 on MMP-2 and MMP-9 activities in mouse fibroblasts. *Journal of the Society of Gynecological Investigation*, *7*, 348–354.
35. Saed, G. M., & Diamond, M. P. (2002). Hypoxia-induced irreversible up-regulation of type I collagen and transforming growth factor-beta1 in human peritoneal fibroblasts. *Fertility and Sterility*, *78*, 144–147.
36. Milligan, D. W., & Raftery, A. T. (1974). Observations on the pathogenesis of peritoneal adhesions: A light and electron microscopical study. *British Journal of Surgery*, *61*, 274–280.
37. Terada, L. S., Guidot, D. M., Leff, J. A., Willingham, I. R., Hanley, M. E., Piermattei, D., & Repine, J. E. (1992). Hypoxia injures endothelial cells by increasing endogenous xanthine oxidase activity. *Proceedings of the National Academy of Science of the United States of America*, *89*, 3362–3366.
38. Snoj, M. (1993). Intra-abdominal adhesion formation is initiated by phospholipase A2. *Medical Hypotheses*, *41*, 525–528.
39. Vikram, D. S., Bratasz, A., Ahmad, R., & Kuppusamy, P. (2007). A comparative evaluation of EPR and OxyLite oximetry using a random sampling of pO₂ in a murine tumor. *Radiation Research*, *168*, 308–315.